Multimed Tools Appl (2018) 77:9595–9620
https://doi.org/10.1007/s11042-017-5321-6

Comprehensive survey on haze removal techniques

Dilbag Singh[1] · **Vijay Kumar**[1]

Received: 21 December 2016 / Revised: 13 August 2017 / Accepted: 19 October 2017/
Published online: 9 November 2017

Abstract Image haze removal techniques are extensively used in several outdoor applications. Lack of sufficient knowledge that is required to restore hazy images, the existing techniques usually use various attributes and assign constant values to these attributes. Unsuitable assignment to these attributes does not provide desired dehazing results. The primary objective of this review paper is to provide a structured outline of some well-known haze removal techniques. This paper also focuses on the methods which can assign optimal values to image dehazing attributes. The review has revealed that the meta-heuristic techniques can attain the optimistic haze removal parameters and also concurrently develops an optimistic objective function to estimate the depth map efficiently. Finally, this paper describes the various issues and challenges of image dehazing techniques, which are required to be further studied.

Keywords Haze removal · Dark channel prior · Filtering · Supervised learning · Meta-heuristic techniques

1 Introduction

Images captured in poor weather conditions may lose their potential information, due to a dirty medium such as particles and water droplets in an atmospheric veil. Thus, these hazy images do not provide enough significant details for future vision applications [57]. Poor illumination decreases the visibility of images. Thus, these images are not suitable for future vision applications such as weather forecasting, radar tracking system, lane detection

✉ Dilbag Singh
dggill2@gmail.com

Vijay Kumar
vijaykumarchahar@gmail.com

[1] Department of Computer Science and Engineering, Thapar University, Patiala, India

system, etc. Therefore, these kinds of applications demand haze removal technique as a pre-processing tool to improve the performance of vision applications under poor environmental conditions [24].

The number of particles available in the atmosphere are fluctuate according to the weather condition. An enormous attempt has been made to quantify the size of these particles as shown in Table 1. Depending upon the category of the visual belongings, poor weather circumstances are categorized into two types: Steady and dynamic [24]. In steady poor weather, ingredient droplets are minimum (1–10 μm) and steadily float in the atmosphere. Haze, mist, and fog are the examples of steady weather conditions. The illumination effect at a given pixel is because of the collective consequence of the high degree of droplets within the pixel's solid angle. In dynamic poor weather circumstances, ingredient droplets are 1000 times more (0.1–10 μm) than steady weather [33]. Snow and rain are the examples of dynamic weather circumstances.

The majority of vision applications provide poor results in case of weather degraded images [3]. Thus, haze removal algorithms become significant for several vision applications like aerial imagery, object recognition, image retrieval and object analysis [42].

In hazy days, illumination observed from a scene is sprinkled and immersed because of the considerable occurrence of molecules and aerosols hanging in the environment [4]. Because of the effect of intense haze, the perceptibility of environment and visibility become poorer considerably, that result in significant disturbance to different vision applications [22]. In haze environment, objects have poor visibility [54] and such images are often recognized as of low contrast and poor intensity [53]. Poor brightness considerably influences the consistency of image processing applications [41].

1.1 Imaging under different weather environments

Figures 1 and 2 demonstrate the imaging procedure. In the haze-free circumstances, the object imitates energy from illumination source such as direct sunlight, diffuse skylight and illuminate reflected by the source. The energy of the input scene is reduced when it arrives at the vision system. Vision system integrates the received energy and centers it onto the image plane. Excluding the haze, images have brighter colors as shown in Fig. 1. In hazy circumstances, the situation turns out to be more difficult (as in Fig. 2) [57].

This review paper has the following structure: Section 2 describes the general framework and mathematical model of the haze removal algorithms. Section 3 describes the comprehensive review on existing well-known haze removal techniques along with their categorization. Comparative analysis of haze removal techniques is given in tabular form in Section 4. In Section 5, the challenges of different haze removal approaches and directions for future research are given. Section 6 describes different quality metrics which can be

Table 1 Weather conditions and associated particle types and sizes

Circumstances	Type	Radius(μm)
Fog	Water droplet	1–10
Cloud	Water droplet	1–10
Haze	Aerosol	10–2
Air	Molecule	10–4
Rain	Water droplet	102–104

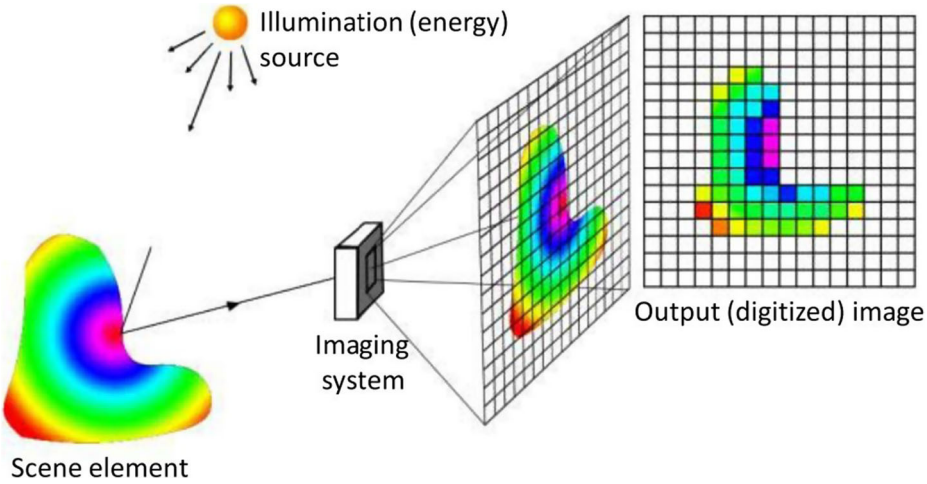

Fig. 1 Procedure of imaging under sunny weather [57]

used to evaluate the performance of haze removal techniques. In Section 7, various applications of haze removal techniques are discussed. The concluding remarks and future scope are presented in Section 8.

2 General framework and mathematical formulation

The existing image enhancement and restoration techniques are not so useful to reduce the effect of haze from hazy images. As known a prior, haze reduces the optical information and thus decreases the accuracy of data analysis. Remotely sensed, underwater and road side images are primarily susceptible to weather effects [22]. The effect of haze increases with the distance, which makes image dehazing a challenging problem. Under poor weather circumstances, the illumination arriving at the visual sensor is harshly sprinkled by the

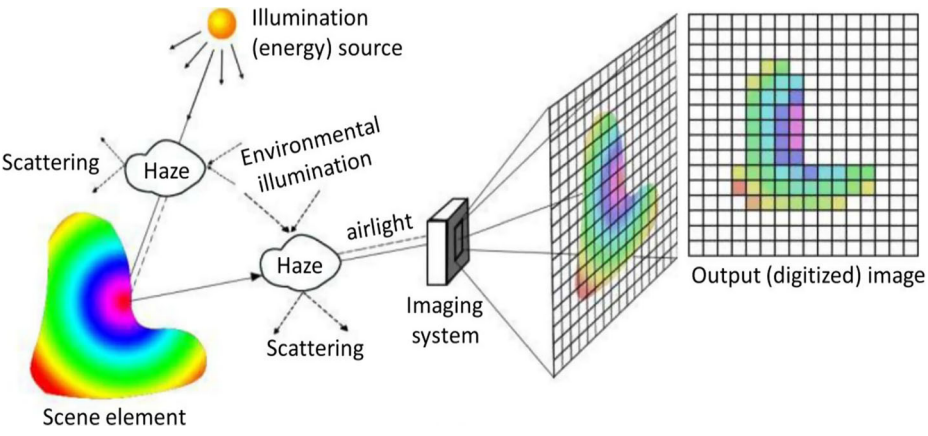

Fig. 2 Procedure of imaging under hazy weather [57]

atmosphere [54]. The resulting decay in brightness differs across the object and is exponential in the depth of object points. Thus, the traditional space invariant vision processing algorithms are not so effective to reduce haze effects from digital images. Therefore, haze removal technique is required to remove the haze from digital images [41].

Several researchers have shown that the effect of haze in digital images increases when the distance from camera and scene increases [41, 54] and [37]. If an input is just a particular hazy image, then an assessment of the depth knowledge is under certain assumptions. Usually, evaluation of depth map demands two images. Thus, numerous techniques have been developed that may utilize several images [52].

However, these techniques are unable to apply on standard vision framework. There are various techniques that can reduce haze by a single image. To improve the estimation of the depth map, these methods utilize certain constrains [34]. A general structure of the haze removal technique is depicted in Fig. 3.

The step by step detail of Fig. 3 is demonstrated by using mathematical models of each step. Table 2 represents various symbols with their respective meanings which are utilized to mathematically describe the steps of the generic framework of haze removal techniques.

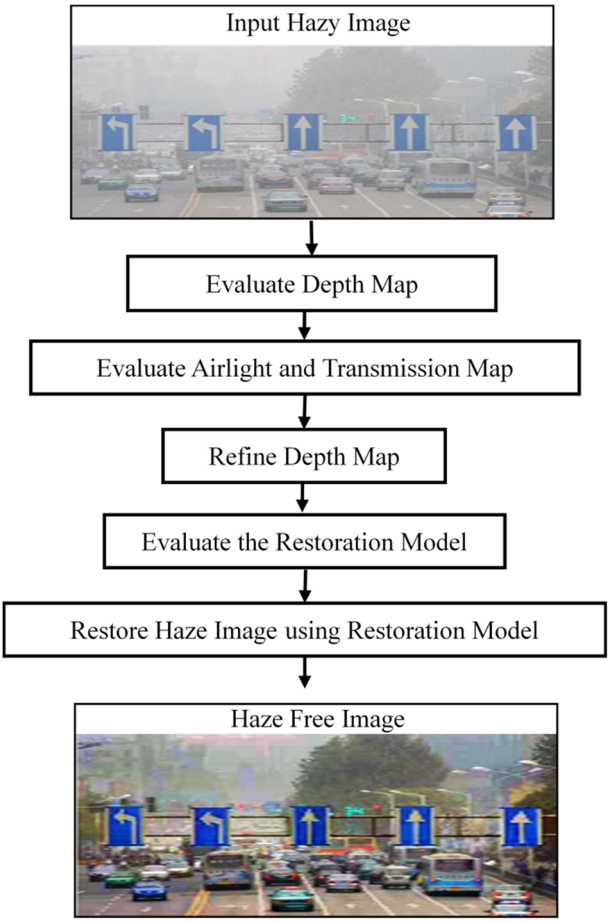

Fig. 3 Generic framework of haze removal techniques

Table 2 Nomenclature used

Symobol	Meaning
A_C	Average contrast
A_{veil}	Atmospheric veil
c_1 and c_2	Constant coefficients for SSIM
cc	Color channel
C_g	Contrast gain
C_{hfi}	Average contrast of haze free image
C_{hi}	Average contrast of haze image
G_{al}	Global atmospheric light
G_d	Guided image
G_{dp} and G_{dq}	Assigned weights in J_{tf}
GT	Ground truth image
G_{val}	Guided image intensity value
I_{cc}	Color image
I_{depth}	Scene depth
I_{mg}	Observed image
I_{st}	Saturation value
I_{val}	Image intensity value
J_{dc}	Dark channel
J_{sr}	Scene radiance
J_{tf}	Joint trilateral filter
k	Pixel position
$K \times L$	Rows and Columns
K_r	Local window
L_b	Lower bound
LC_0, $LC_1$and LC_2	Unknown liner coefficients
max	Maximum intensity
M_{cc}	Transmission veil of $\min_{cc}$
$\min_{cc}$	Minimum color channel
min	Minimum intensity
M_{tx}	Medium transmission
$\|n\|$	Number of pixels in the window
$\mathcal{O}(k)$	Local patch centered at k
OP	Haze free image
(p, q)	Pixel positions
R_r	Random error
S_{ac}	Surface albedo coefficient
S_{bt}	Scene brightness
S_f	Shading factor
S_p	Saturated pixels
z	Local color component
α	Constant coffiecient for J_{tf}
μ	Mean
σ^2	Variance
${\sigma_p}^2$and${\sigma_q}^2$	Sample variances at pixel i and j
σ_{pq}	Sample cross-covariance

2.1 Depth map estimation

Figure 4 shows the effect of light on outdoor images. This figure clearly represents that the effect of haze on outdoor images increases as the distance of scene becomes larger. A hazy image formed as shown in Fig. 4 can be mathematically modeled as follows.

The haze removal techniques demand the estimation of a depth map. The evaluated depth map can be used to evaluate the airlight and transmission map. Many developed methods have predicted the depth map by using the scene characteristics. These features can be shading technique, human visual function, or illuminate based function. Following are some well-known methods which have been used so far by researchers to estimate the depth.

2.1.1 Optical model

The classical hazy image formation model i.e., optical model is proposed by Cozman and Krotkov [8] and given as in (1):-

$$I_{mg}(k) = J_{sr}(k)M_{tx}(k) + G_{al}(1 - M_{tx}(k)) \tag{1}$$

where I_{mg} is the observed image intensity, J_{sr} is the scene radiance, G_{al} is the global atmospheric light and k is the pixel position. The medium transmission, M_{tx}, is an exponential function of distance between object and camera, describing the portion of light i.e., not scattered but directly reaches the camera [14]. This model is widely applied in computer vision and the objective of image haze removal is to recover scene radiance J_{sr} from observed image intensity I_{mg}, estimated atmospheric light G_{al} and transmission M_{tx}.

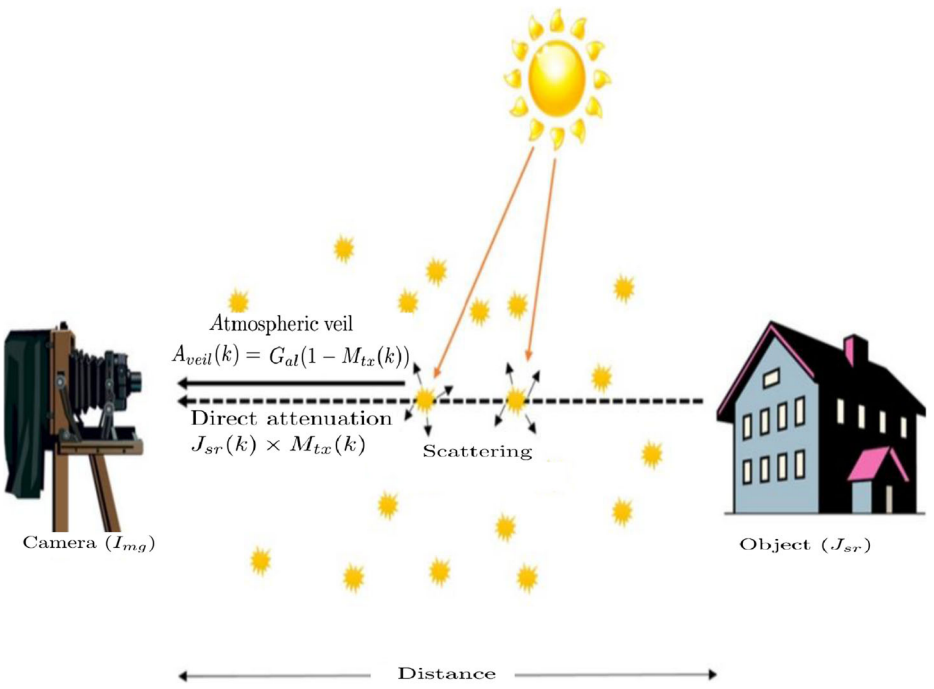

Fig. 4 Haze imaging model

2.1.2 Refined optical model

Fattal [43] proposed a refined image formation model by replacing the unknown image J_{sr} with a product, $S_{ac} \times S_f$, where S_{ac} is the surface albedo coefficient and S_f *is* the shading factor. In this model, both the surface shading and transmission functions are taken into consideration. The ambiguities faced by traditional single image de-hazing methods, were solved by searching for a solution, in which the resultant shading and transmission functions are not similar with each other. Using the same principle, the atmospheric light can be estimated.

2.1.3 Visibility restoration

Instead of calculating image transmission M_{tx}, the atmospheric veil $A_{veil}(k) = G_{al}(1 - M_{tx}(k))$ was introduced to avoid the separation between the medium extinction coefficient and the scene distance depth [44]. These two factors, which are not always possible to calculate, influence the transmission. Therefore, the image formation model can be rewritten as follows:

$$I_{mg}(k) = J_{sr}(k)\left(1 - \frac{A_{veil}(k)}{G_{al}}\right) + A_{veil}(k) \tag{2}$$

White balance was initially adopted to set airlight M_{tx} to $[111]^T$ and the observed image I_{mg} was normalized. Therefore, the atmospheric veil $A_{veil}(k)$, rather than the transmission, is required to be calculated for image restoration.

2.1.4 Dark channel prior

The Dark Channel Prior assumption proposed by He [22] is based on observations about haze-free images, in which there is at least one color channel with some pixels whose intensities are very low or close to zero. In dark channel prior based approaches, the image formation model used is the traditional one (1) and the dark channel J_{dc} is calculated as follows:

$$J_{dc} = \min_{z \in \mathcal{O}(k)} \left(\min_{cc \in RGB} \left(J_{sr}^{cc} \right) \right) \tag{3}$$

where cc is a color channel of J_{sr} and $\mathcal{O}(k)$ is a local patch centered at k. The two minimum operators are commutative. Both transmission M_{tx} and atmospheric light G_{al} can be obtained through the dark channel prior based method.

2.1.5 Learning based color attenuation prior

Instead of searching for the transmission $M_{tx}(k)$, Zhu [57] introduced a novel color attenuation prior to obtaining the scene depth $I_{depth}(k)$. A linear model was employed to relate $I_{depth}(k)$ with scene brightness $S_bt(k)$ and saturation $I_{st}(k)$, which can be mathematically written as follows:

$$I_{depth}(k) = LC_0 + LC_1 S_b(x) + LC_2 I_{st}(k) + R_r(k) \tag{4}$$

where LC_0, LC_1 and LC_2 are three unknown linear coefficients, to be obtained through the supervised learning method, R_r is the random error of this model and R_r can be regarded as a random image. This random error is assigned with a Gaussian density, which gives $R_r(k)$

$\in N(0, \sigma^2)$. Furthermore, 500 haze-free images were used in [57] as the training samples, and the Maximum Likelihood Estimation method was adopted to achieve the best learning results, which is $LC_0 = 0.12$, $LC_1 = 0.95$, $LC_2 = 0.78$ and $\mu = 0.04$.

2.2 Depth map refinement

Depth map refinement is a technique which reduces the errors of depth map form haze, noise, poor defined edges or other undesired artifacts. Filtering is a well-known method to refine the depth map. The subsequent section demonstrates the mathematical model of Joint Trilateral Filter (JTF), [37]. As in [37, 44] have set $A^{cc}_{viel}(k) = G_{al}(1 - M_{tx}(k))$ as the transmission veil, $M_{cc}(k) = \min_{cc}(I_{cc}(k))$ is the min color components of $I_{mg}(k)$. As known a prior, $0 \leq A_{veil}(k) \leq M_{cc}(k)$, thus for gray scale image, $M_{cc} = I_{mg}$. JTF [37] have computed the $T_{xf}(k) = median(k) - J^{tf}_{\mathcal{O}}(|M_{cc} - median(k)|)$. And then, [37] have acquired it by $A_{veil}(k) = \max\left(\left(\min\left(\alpha T_{xf}(k), M_{cc}(k)\right)\right), 0\right)$. Here, α is the parameter in (0,1). Finally, the transmission of each patch can be written as follows:

$$\overline{\mathrm{M_{tx}}} = 1 - \frac{A_{veil}}{G^{cc}_{al}} \tag{5}$$

The background G^{cc}_{al} is usually assumed to be the pixel intensity with the highest brightness value in an image. However, in practice, this simple assumption often renders erroneous results due to the presence of self-luminous organisms. Consequently, the authors [37] computed brightest pixel value among all local min corresponding to the background light G^{cc}_{al} as follows:

$$G_{al} = \max_{z \in I_{mg}} \left(\min_{z \in \mathcal{O}(k)} \left(I^{cc}_{z} \right) \right) \tag{6}$$

where $I^{cc}_{mg}(z)$ is the local color components of $I_{mg}(k)$ in each patch.

JTF can overcome the gradient reversal artifacts occurring. The filtering process of JTF is first performed under the guidance of the image (G_d). In JTF, input image (I_{mg}) itself is taken as G_d. Let I_{val} and G_{val} be the intensity values at pixel q of the minimum channel image and guided input image respectively. W_r be the kernel window centered at pixel k. JTF is then formulated by follows:

$$J_{tf}(I_{mg}) = \frac{1}{\sum_{q \in K_r} M_{cc_{pq}}(G_d)} \left(\sum_{q \in k_r} M_{cc_{pq}}(G_d) I_q \right) \tag{7}$$

Here, the kernel weights function $M_{cc_{pq}}(G_d)$ can be written as follows:

$$M_{cc_{pq}}(G_d) = \frac{1}{|n|^2} \sum_{n:(p,q) \in k_r} \left(1 + \frac{(G_{dp} - \mu_n)(G_{dq} - \mu_n)}{\sigma_n^2 + \epsilon} \right) \tag{8}$$

where mu_n and σ_n^2 are the mean and variance of G_d in local window k_r, respectively. $|n|$ is the number of pixels in this window. When both G_{dp} and G_{dq} are on the same side of an edge, the weight assigned to pixel q is large. When G_{dp} and G_{dq} are on different sides, a small weight will be assigned to pixel q.

2.3 Restoring the haze-free image

After refining the depth map, it is just required to restore the hazy image using haze removal restoration function. After refining the transmission map, the scene radiance can be mathematically recovered as follows:

$$J_{sr}(k) = \frac{I_{mg}(k) - G_{al}}{\max(M_{tx}(k), L_b)} + G_{al} \tag{9}$$

where L_b is a lower bound whose typical value is 0.1 that is introduced to make this algorithm more robust to noise.

3 Haze removal techniques

This section contains comprehensive review on existing well-known haze removal techniques. The categorization of these techniques is also done. The categories of image dehazing techniques are shown in Fig. 5. Haze removal methods are divided into seven broad categories i.e. (1) Depth estimation based haze removal, (2) Wavelet based haze removal, (3) Enhancement based haze removal (4) Filtering based haze removal, (5) Supervised learning based haze removal, (6) Fusion based haze removal and (7) Meta-heuristic techniques based haze removal. The subsequent section contains the details of various haze removal methods along with their strengths and weaknesses.

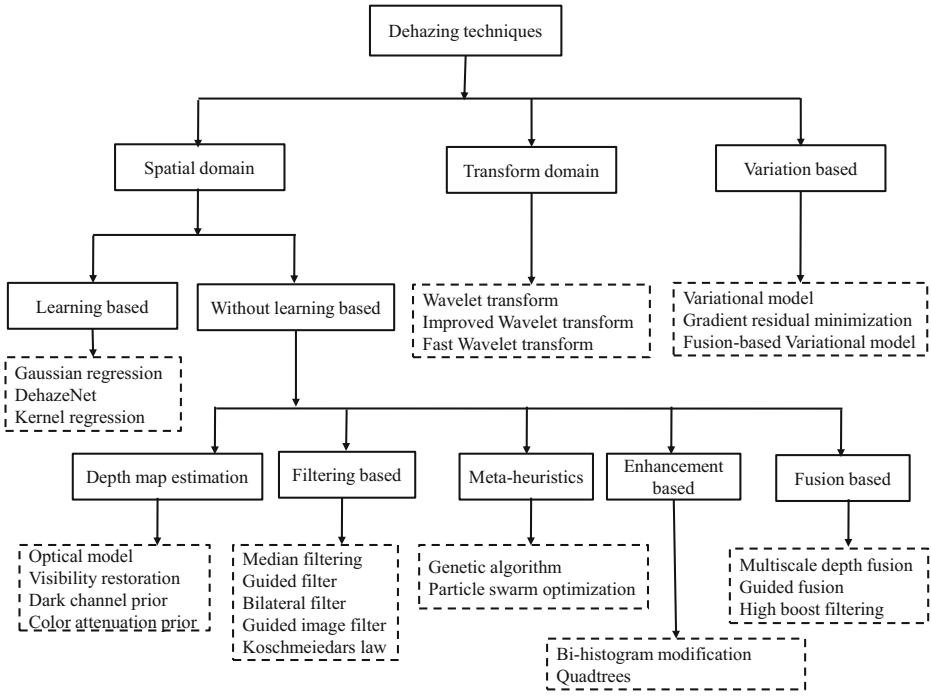

Fig. 5 The categories of image dehazing techniques

3.1 Depth estimation based haze removal

The multi-scale tone strategy is utilized to evaluate the atmospheric veil in an optimistic way. Thus, it can manipulate the quality and illuminate of an input image at multiple scales [56]. But, this technique experiences the same issue of the majority of haze-free techniques i.e., it does not attain consistent results, especially for heavy haze images. It performs poorly, whenever it fails to recognize local maxima and minima precisely.

Due to a maximum intensity of airlight, existing methods select pixels with the greatest intensity to evaluate the airlight map. However, some pixels with heavy illuminate are also produced by some other light foundations, such as train headlights. The Gaussian distribution based haze removal technique selects the airlight contenders from the brightest segment of haze image. The color similarity assessment is also utilized to hierarchically filter the airlight contenders. In the end, mean color from filtered airlight contenders is utilized for airlight estimation [6]. In [19], fast haze removal technique is introduced. This model can evaluate the atmospheric light by utilizing an infinite sky area and close white area. However, it still suffers from the edge preservation issue, because the potential edges may degrade during the haze free process.

Change of detail prior is utilized in [29] which can remove the haze from an image by utilizing multiple scattering occurrences in the dissemination of illumination. By using this technique, a thickness of haze can be evaluated successfully to restore a haze-free image. The change of detail prior is stable to local areas of haze image which contain objects in dissimilar depths [29]. However, it cannot preserve the edges of the haze free images.

A superpixel technique is designed for evaluating the transmission on sky as well as non-sky areas, to diminish the effect of halo artifacts around edges and the decreases the color distortion in the sky area. Thus developed technique can overcome the halo artifacts issues with most of the existing haze removal techniques. [50]. However, this technique can be improved further by efficiently estimating the atmospheric veil, to restore the image in more consistent manner.

3.2 Wavelet based haze removal

The improved wavelet transform technique for proficient image haze removal is proposed by [36]. This technique initially utilizes wavelet transform for removing the haze from image, and then retinex technique is utilized to improve the color performance and to enhance the color effect after implementing the wavelet transform for image haze removal.

The improvement in the dark channel prior is done by utilizing the wavelet transform in [55]. This technique applies wavelet transform and guided filter to evaluate and improve the depth information of hazy images. Also contrast enhancement techniques are utilized as pre-processing techniques to recover the illuminate of hazy image.

Fast wavelet transform technique is proposed for improving the speed of haze removal technique without considering any prior knowledge. This method concurrently removes haze from the image and improves sharpness of the image. In the haze removing stage, two coarse transmission maps using dark channel prior are fused. One is obtained based on single-point pixel and the other is obtained by patch. For the sake of dehazing and enhancing sharpness simultaneously, a modified fast wavelet transform based unsharp masking framework is applied to control the effectiveness of sharpness by constructing a sigmoid function adaptively [48].

3.3 Enhancement based haze removal

In this section, various haze removal techniques are discussed which are based upon several image enhancment techniques. The dark channel prior utilizes soft matting technique that requires more memory and time. Thus, dark channel prior is efficient for small size images only. To overcome this issue, soft matting is replaced by adaptively subdivided quadtrees built in image space. The quadtree improves the speed by converting the problem of solving a N-variable linear model of soft matting, to a much lesser m-variable linear model, where N is number of pixels and m is number of corners in quadtree. Therefore, quadtrees considerably decrease both space and time cost while still preserve visual reliability [9].

3.4 Filtering based haze removal

The gamma correction and median filtering by utilizing look up table that can determine the haze free images in proficient way. This method has minimum computation time than existing techniques without losing the brightness of the haze free image [26]. Because this method cannot preserve the edges of haze free images.

L2-norm based haze removal method can evaluate the depth by calculating average vector L2-norm of sample window. After that it filters the evaluated transmission map by utilizing a guided filter. Thus, it uses the guided filter to preserve edges of haze free image [10]. However, it still suffers from the halo artifacts issue, which may introduce during fusion process. The weighted guided image filter utilizes an edge aware weighting to improve the guided image filter further. This method has overcome the problem of halo artifacts with the help of guided image filter. Weighted guided image filter has minimum computation time than existing techniques without losing the brightness of the haze free image [30]. The bilateral filter is utilized in order to attain local smoothness and as well as edge preservation of haze free image. This technique reduces the adverse effects due to difference in evaluating the global atmospheric illuminate [42]. The bilateral filter suffers from the halo artifacts issue, which may introduce during the fusion process. The weighted guided image filter and Koschmiedars law [28] without using any prior is utilized to simplify the dark channel of haze image into a base and detail layer. The transmission map is evaluated using the base layer, and it is utilised to recover haze free image. But, this method has poor computation time than majority of existing techniques.

3.5 Supervised learning based haze removal

By developing a linear model with supervised learning technique, depth of haze image can be evaluated in more consistent way than most of existing techniques. By using this depth information one can easily evaluate the transmission map and therefore recover the scene brightness by utilizing the atmospheric scattering method. [57]. But, for supervised filtering a lot of hazy and haze free images of the dissimilar scenes and environments are required which make it difficult for real time implementation.

Supervised learning based techniques typically require well-designed models and also require dummy hazy images for estimating the haze depth in efficient way. But, it cannot always contain significance depth knowledge of the natural images in practice. The two layer Gaussian regression [12] is proposed to overcome this issue. By utilizing training hazy

and haze free image, the two layer Gaussian regression found an direct association among haze image and its depth knowledge.

A trainable end-to-end system called DehazeNet [2] is proposed for efficient monitoring of the medium transmission. DehazeNet can significantly estimate the transmission map by using the atmospheric scattering method. DehazeNet implements standard artificial neural network to estimate the transmission map from the hazy image. A nonlinear activation function is also considered in DehazeNet, called bilateral rectified linear unit, which has an ability to enhance the quality of restored haze free image.

The transmission estimated by dark channel prior is not smooth and possesses no local neighbor information which leads to the block effects. An improved haze removal method is proposed using Kernel Regression Model on local neighbor data. In this approach firstly, the initial transmission in atmospheric light model is estimated by dark channel prior. Secondly, the transmission is refined according to Kernel Regression Model. Then restoration model comes in action to remove the effect of haze from the image [52].

3.6 Fusion based haze removal

A multiscale depth fusion technique is described for removing the haze from single image [47]. The results of multiscale filtering are probabilistically combined into a fused depth map depending upon the model. The fusion is devised as an energy minimization issue that integrate spatial Markov dependence. The multiscale depth fusion technique can estimate the depth map in more consistent way and also has the ability to preserve the edges of haze free image with sharp details.

An efficient technique for transmission map estimation by using the guided fusion is presented in [35]. By utilizing the reliability guided fusion of block-level and pixel-level dark channels, a high-quality refined transmission map is evaluated. This technique successfully reduces the dark channel prior failure probability and haloes by growing the mask size in an edge-preserving manner. Dark channel prior failure in the sky (bright) regions is handled by limiting the contrast boost of sky-like surfaces. Thus it produces a more natural recovery of the sky regions.

A fusion strategy based haze removal technique is proposed in [32], which fuses the outcomes of the linear transform with the guided image filtering. Main steps of the algorithm are as follows. First, the first input image of the fusion process is obtained via a simple linear transformation. Second, an improved high-boost filtering algorithm based on guided image filtering is proposed to obtain the second input image of the fusion process. Third, a simple fusion method is used to fuse the above two input images. The final dehazing result is obtained by a simple white balance process. This algorithm not only greatly enhances the visibility of outdoor image, but also has high computational efficiency.

3.7 Meta-heuristic techniques based haze removal

Most of existing haze removal technique are unable to select best parameters for better haze removal. Therefore, does not provide optimistic results. The use of genetic algorithm for haze removal is that the parameter selection and function maximization can be strongly related issues. The genetic algorithm can attain the optimistic haze removal parameters by using contrast gain as fitness function [20]. However, genetic algorithm does not guarantee the global optimal solution, therefore requires its hybridization with others.

Haze Removal from the Noise Filtering Perspective is proposed by [31]. Images contaminated by haze in the form of noise possess two main characteristics: high intensity and

low saturation. Therefore, a weighted sum of input image intensity and saturation is used to describe the haze severity. Atmospheric light can be estimated by the same principle, while a small correction is needed when images contain over-bright objects. After the two weighted maps are constructed, local statistics of the severity map are applied in image noise filtering. Four parameters involved are optimized via particle swarm optimization. The objective function, in this work, is to maximize the saturation of output image. Furthermore, a penalty function to control the hue change is introduced while calculating the overall fitness.

3.8 Variational image dehazing

Existing dehazing approaches estimate depth map to remove the haze from images. Thus, these techniques are vulnerable to failure whenever the physical assumptions are violated. Image enhancement techniques do not evaluate the depth map. Therefore, these techniques do not suffer from this issue. However, these suffer from the over-enhancement issue. Fortunately, variational image dehazing technique can overcome the physical assumptions failure issue and over-enhancement problem. Succeeding section describes some well-known variational image dehazing techniques [17].

Fang et al. [13] have designed a unified variational technique to restore hazy images and to remove noise from a single image. Total variation regularization is utilized as energy model for dehazing. Negative gradient descent technique is implemented to handle the corresponding Euler-Lagrange equations. To evaluation efficient initial attributes, the depth map is also improved with windows adaptive technique based on DCP which can remove the block artifacts. Galdran et al. [17] utilized a perceptually inspired variational based dehazing technique to develop an energy minimization model. The energy model is dependent upon a hazy image under a gray-world assumption. This assumption is further improved by estimating a average value for a dehazing image, and a local contrast evaluation is involved in the designed model. This technique outperforms in terms of visible edges in local areas. However, dark masks as a kind of unwanted artifacts, may be found in close-range areas.

Chen et al. [5] designed a dehazing technique for reliable suppression of several artifacts in images. Initially, the depth-edge-aware smoothing technique is implemented to improve the initial atmosphere veil estimated using local priors. In the image restoration step, Gradient Residual Minimization is implemented for jointly remove the haze from image while explicitly decreasing the various artifacts. Galdran et al. [18] designed fusion-based variational image-dehazing method. Fusion based variation dehazing does not rely on a physical model from which to estimate a depth map, nor does it require a training stage on a database of human-labeled examples.

4 Comparative analysis of haze removal techniques

In this section, comparisons have been shown among existing techniques by considering the various attributes.

Table 3 contains the comparison of existing techniques based upon certain features and artifacts. It clearly shows that each technique has its own features and limitations. No technique is effective for every case of haze removal. Thus it shows haze removal is still an open area of research.

Ranking a hazy algorithm is difficult task, because various kinds of vision applications may focus on different issues. Such as real time applications may demand dehazing techniques with good speed, Remote sensing image processing systems demand dehazing

Table 3 Comparative analysis of existing haze removal techniques

Ref.	Year	Technique	Edge preservation	Speed	Color distortion	Halo artifacts	Large haze gradients
[14]	2008	Optical model	No	Average	Yes	No	No
[44]	2009	Fast visibility restoration	No	Good	Yes	No	No
[51]	2010	Multi-scale retinex	No	Good	Yes	No	No
[13]	2010	Variational dehazing	Yes	Average	No	No	Yes
[22]	2011	Dark channel prior	No	Poor	Yes	No	No
[25]	2013	Bilateral filter	Yes	Poor	No	No	No
[9]	2013	Quadtrees	Yes	Good	No	No	No
[41]	2013	Physical model	No	Poor	Yes	No	No
[37]	2014	Joint trilateral filter	Yes	Good	No	No	No
[23]	2014	Visibility enhancement	No	Average	No	No	No
[48]	2014	Fast image enhancement	No	Average	Yes	No	No
[36]	2014	Improved wavelet transform algorithm	Yes	Good	No	No	No
[15]	2014	Dehazing using color-lines	No	Average	No	No	No
[47]	2014	Multi-scale depth fusion	Yes	Average	No	Yes	Yes
[49]	2015	Canonical correlation	No	Good	No	Yes	Yes
[3]	2015	Bi-histogram modification	No	Good	No	No	Yes
[30]	2015	Weighted guided image filter	Yes	Good	No	Yes	No
[34]	2015	Deformed haze model	Yes	Average	No	Yes	No
[28]	2015	Edge preserving	Yes	Average	No	Yes	Yes
[29]	2015	Change of detail prior	Yes	Average	No	No	Yes
[19]	2015	Linear transformation	No	Good	No	Yes	Yes
[6]	2015	Hierarchical airlight estimation	Yes	Average	No	No	Yes
[26]	2015	Look-up-table	No	Good	No	Yes	Yes
[57]	2015	Color attenuation prior	Yes	Average	No	No	Yes
[16]	2015	Improved dark channel prior	No	Good	No	Yes	Yes
[17]	2015	Improved Variational dehazing	Yes	Average	Yes	No	Yes
[50]	2016	Multiple scattering model	No	Average	No	Yes	Yes
[4]	2016	Intervention refinement filter	No	Average	No	Yes	Yes
[20]	2016	Genetic algorithm	Yes	Average	No	Yes	Yes
[2]	2016	DehazeNet	Yes	Average	No	Yes	Yes
[5]	2016	Depth-edge-aware Variational model	Yes	Average	No	Yes	Yes
[52]	2016	Kernel regression model	Yes	Good	No	Yes	Yes
[12]	2016	Gaussian process regression	Yes	Good	No	Yes	Yes
[31]	2016	Noise filtering	Yes	Average	No	Yes	Yes
[35]	2016	Guided fusion	Yes	Good	No	Yes	Yes
[32]	2016	High boost filtering based fusion	Yes	Good	Yes	Yes	Yes
[18]	2017	Fusion based Variation model	Yes	Average	No	Yes	Yes

technique with lesser artifacts and large haze gradient, and some other outdoor applications may demand the removal of haze from hazy images with large haze gradient. However, we have given the highest rank to dehazing technique that cover almost all the issues at a same time.

Table 4 contains the comparison of existing techniques based upon their respective ranks. Among the existing dehazing techniques, High boost filtering based fusion has the highest rank among other techniques.

Table 5 summarizes the pros and cons of several typical image dehazing techniques.

5 Challenges and future directions

In hazy weather, water droplets float in the atmosphere. These droplets are extremely tiny in size. Thus, image illuminate developed at a pixel is the integrated effect of the maximum numbers of water droplets inside the pixels solid angle. The energy reflected by the object's surface is not only attenuated by the overhanging water droplets but also merges with airlight when it perceived by the viewer. Thus, qualtiy of the captured image is not so significant as in haze free image. The primary objective of haze removal techniques is to restore color and significant details of the image. Attenuation and airlight are primary functions of distance of scene from the camera. Therefore, haze removal techniques require depth information of the hazy image. In real time applications, it is required to estimate the depth information. But, estimating the depth map is challenging issue, because the airlight attenuation ambiguity holds for every pixel and cannot be determined autonomously. Therefore, to handle ambiguity issue, an assumption or prior information is required [45]. The subsequent section contains various challenges associated with the haze removal techniques.

5.1 Atmospheric light monitoring

The atmospheric light is reliably monitored by using the dark channel prior, particularly when the dark channel is evaluated by utilizing a large local mask. Thus, if the local mask size utilised in dark channel evaluation is not sufficiently large, it is suggested to employ an supplementary dark channel with a larger local mask size only for atmospheric light monitoring. The utilization of local entropy is also found to be useful in improving the monitoring accuracy because atmospheric light monitoring from intense objects can be prohibited [27].

5.2 Over enhancement

Enhancement of the hazy image is found to be critical task because of the complexity in restoring the illuminate and color while holding the color reliability. During enhancement of hazy images, over enhancement leads to saturation of pixel value. Thus, enhancement should be restricted by several assumptions to avoid saturation of image and maintain suitable color reliability.

5.3 Large haze gradients

The primary drawback of majority of existing methods is that they may lose significant details of restored images with large haze gradients.

Table 4 Ranking of existing haze removal techniques

Ref.	Technique	Ranking based upon Speed	Ranking based upon Artifact removal	Ranking based upon Large haze gradients	Overall rank
[32]	High boost filtering based fusion	1	1	1	1
[28]	Edge preserving	2	4	3	2
[35]	Guided fusion	4	3	4	3
[12]	Gaussian process regression	3	2	2	4
[52]	Kernel regression model	5	7	8	5
[20]	Genetic algorithm	6	5	7	6
[2]	DehazeNet	9	6	6	7
[5]	Depth-edge-aware Variational model	7	10	5	8
[31]	Noise filtering	8	8	11	9
[18]	Fusion based Variation model	10	11	9	10
[17]	Improved Variational dehazing	12	12	10	11
[49]	Canonical correlation	13	9	13	12
[19]	Linear transformation	11	15	12	13
[6]	Hierarchical airlight estimation	14	13	15	14
[26]	Look-up-table	15	14	16	15
[16]	Improved dark channel prior	17	18	14	16
[50]	Multiple scattering model	18	16	19	17
[44]	Fast visibility restoration	16	17	18	18
[51]	Multi-scale retinex	19	20	17	19
[36]	Improved wavelet transform algorithm	20	21	20	20
[9]	Quadtrees	23	19	21	21
[41]	Physical model	21	22	23	22
[37]	Joint trilateral filter	22	25	22	23
[30]	Weighted guided image filter	24	23	25	24
[13]	Variational dehazing	26	24	24	25
[57]	Color attenuation prior	25	26	28	26
[4]	Intervention refinement filter	28	28	26	27
[34]	Deformed haze model	30	27	27	28
[47]	Multi-scale depth fusion	27	30	33	29
[14]	Optical model	31	31	32	30
[48]	Fast image enhancement	29	29	34	31
[29]	Change of detail prior	32	34	29	32
[3]	Bi-histogram modification	33	32	30	33
[22]	Dark channel prior	36	33	31	34
[25]	Bilateral filter	35	35	37	35
[23]	Visibility enhancement	34	36	35	36
[15]	Dehazing using color-lines	37	35	36	37

Table 5 The comparison of several typical image dehazing techniques

Technique	Pros	Cons	Applications
Optical model [14]	(a) Signficant results for thin haze	(a) Transmission and surface shading are locally uncorrelated. (b) The absence of multiplicative variation in significant portions.	Natural images
Visibility restoration [44] and [49]	(a) Good speed	(a) Edge preservation is not considered. (b) Not effective for large haze gradients	Lane-marking extraction
Multi-scale retinex [51]	(a) No user interaction is needed. (b) Faster speed	(a) Halo artifacts. (b) Not effective for large haze gradients	Natural images
Dark channel prior [22], [54] and [53]	(a) High-quality haze-free image	(a) Failure in the sky (bright) regions. (b) Fail to restore image under inhomogenious haze. (c) Edge preservation is not considered.	Outdoor images
Image enhancement [48], [3], [9] and [23]	(a) No color distortion (b) Poor speed	(a) Edge preservation (b) Noise suppersion (c) Over/under enhancement	Intelligent transportation vision system
Filtering [30], [37], [10], [42] and [25]	(a) Efficient noise supperssion (b) Edge preservation	(a) Poor speed (b) Halo artefacts (c) Not effective for large haze gradients	Underwater image enhancement
Deformed haze model [34] and [6]	(a) No color drift	(a) May introduce certain artifacts (b) Fail to dehaze image with large haze gradient (c) Sometimes may lead over/ under enhance results	Remotly sensed images
Edge preserving [28]	(a) Efficient edge preservation (b) Low color distortion	(a) Poor computation time	Natural images
Change of detail prior [29]	(a) Stable to local areas	(a) Cannot preserve the edges (b) Color distortion	Natural images
Linear transformation [19]	(a) Efficient for sky area (b) Efficient speed	(a) Potential edges may degraded	Natural images
Look-up-table [26]	(a) Minimum computation time (b) Efficient brightness	(a) Edge preservation (b) Color distortion	Natural images
Multiple scattering model [50]	(a) Decreases the color distortion in sky area (b) Ability to overcome the halo artifats	(a) Not efficient for estimating the atmospheric veil	Natural images
Intervention refinement filter [4]	(a) Edge preservation (b) High contrast	(a) Halo artifacts (b) Lower computational speed	Natural images

Table 5 (continued)

Technique	Pros	Cons	Applications
Meta-heuristic techniques [31] and [20]	(a) Optimistic results	(a) Premature convergence (b) Local optima	Natural images
Superwised learning [12], [52], [57] and [2]	(a) Efficient for all kind of images	(a) Large set of images required for training (b) Learning models are complex and leads to a lower computational speed	Natural images
Wavelet transform [36], [48] and [16]	(a) Effcient noise supperssion (b) Edge preservation	(a) May introduce certain artifacts (b) Fail to dehaze image with large haze gradient (c) Sometimes may lead over/ under enhance results	Natural images
Fusion based [35], [32] and [47]	(a) Have more efficient results than single image dehazing technique.	(a) Models are complex and leads to a lower speed.	Natural images
Variational model based [13], [17], [5] and [18]	(a) Overcome the physical assumptions failure issue (b) over-enhancement problem	(a) Models are complex and leads to a lower speed.	Natural images

5.4 Adaptive parameters selection

Since most of dehazing algorithms may produce oversaturated or undersaturated intensity values due to manual parameter selection. Generally these parameters are patch size, restoration value, lower bound and white balance factor. The majority of existing haze removal techniques has taken these values manually, which depends upon the given set of images. This limits the performance of haze removal as restoration value needs to be adaptive as the effect of haze on given image varies scene to scene and atmospheric veil.

5.5 Meta-heuristic algorithms

The use of meta-heuristic algorithms to adaptively find the haze restoration parameters is ignored by majority of existing researchers. [20] have utilized Genetic algorithm to optimistically find the haze restoration parameters. But, the Genetic algorithm suffers from local optima issue and premature convergence issue. Also particle swarm optimization [31] based haze removal technique suffers from premature convergence and also initial amount of particles limits the performance of the particle swarm optimization. Thus, it is required to explore and apply other meta-heuristic techniques to restore the hazy images.

6 Performance metrics

Performance metrics are used to analyze the quality of an haze removal algorithms. In haze removal techniques, quality metrics are divided into two parts i.e., when ground truth image is given and when ground truth image is not given.

6.1 When ground truth image is given

In this case a ground truth image also called reference image is given in advance. It is an actual haze free image of the same hazy image. However, actual haze free images are only given when someone want to validate its haze removal algorithm on standard hazy images data sets. For objective evaluation of haze removal techniques when reference image is given, several quality metrics can be considered like Mean Squared Error (MSE), Peak Signal to Noise Ratio (PSNR), and Structural Similarity Index Metric (SSIM).

6.1.1 Mean Square Error

The Mean Square Error (MSE) is an error measure, which is utilised to evaluate the difference between the Ground Truth (GT) image and the Haze free image (OP) produced by given algorithm. It is basically a positive integer which ranges from 0 to ∞. Close to 0 is required. MSE can be calculated as follows [1, 40]:

$$MSE = \frac{1}{K \times L} \sum_{q=1}^{K} \sum_{p=1}^{L} [GT(p,q) - OP(p,q)]^2 \tag{10}$$

$GT(p,q)$ represents pixel intensities of ground truth image whereas $OP(p,q)$ depicts the pixel value of haze free image. Also p and q represents the pixel's coordinate values

6.1.2 Peak signal to noise ratio

With respect to haze free image, Peak Signal to Noise Ratio (PSNR) evaluates mean squared error after applying haze free technique. Maximum PSNR value represnts that haze is removed proficiently. Similarly, lesser PSNR value represents poor capability of haze free technique. PSNR can be evaluated as follows [1, 40]:

$$PSNR = 10\log_{10}\left(\frac{255^2}{MSE}\right) \tag{11}$$

6.1.3 Structural similarity index metric

Structural Similarity Index Metric(SSIM) evaluates degree of relationship among hazy and haze free image. SSIM was designed to have a quality reconstruction measure which also considers the relationship of edges (high frequency content) that was not there in case of PSNR. SSIM always lies between 0 and 1. Closer to 1 means higher structural quality of haze free image. It is used to evaluate the structural similarity of edges among GT and OP image. SSIM can be calculated as follows [40]:

$$SSIM(p,q) = \left(\frac{2\mu_p\mu_q + c_1}{\mu_p^2 + \mu_q^2 + c1}\right)\left(\frac{2\mu_{pq} + c_2}{\sigma_p^2 + \sigma_q^2 + c2}\right) \tag{12}$$

In (12) p and q represents the pixel coordinates. Also μ_p and μ_q are sample means of p and q respectively. σ_p^2 and σ_q^2 are the sample variances of p and q, and σ_{pq} is the sample cross-covariance between p and q. The default values for c_1 and c_2 are 0.01 and 0.03, respectively.

6.2 When ground truth image is not given

In real time applications, ground truth images are not given. Then, it becomes difficult to measure the effectiveness of the given algorithm. In case of haze removal techniques, a haze free image has more contrast compared to hazy image. Therefore, contrast gain (Ω) and Percentage of saturated pixels (PSP) can be effective parameters for evaluating the best haze removal technique.

6.2.1 Contrast gain

Contrast gain (Ω) is defined as the average contrast difference between hazy and haze-free image [45]. Higher the value of Ω indicates that the given dehazing technique is more efficient than others. Assume AC_{hfi} and AC_{hi} are average contrast values of haze free and hazy image respectively, then Ω can be computed as follows [38, 39]:

$$\Omega = AC_{hfi} - AC_{hi} \tag{13}$$

Assume an image of size $K \times L$ can be represented by $I_\kappa(K, L)$. Then, average contrast AC can be computed as follows:

$$AC = \frac{1}{K \times L}\sum_{p=1}^{K}\sum_{q=1}^{L} I_\kappa(p,q) \tag{14}$$

6.2.2 Percentage of saturated pixels

The Contrast gain (Ω) should not be so high that the pixels of haze free image become saturated. Therefore, the Percentage of saturated pixels (τ) is needed to be computed [45]. τ can be mathematically represented as follows [38, 39]:

$$\tau = \frac{S_p}{K \times L} \tag{15}$$

Here, S_p represents the number of pixels that are saturated either completely black or white, after the haze removal technique, which were not present in the hazy image. The lower value of τ indicates the given dehazing technique is better than others.

6.2.3 Visible edges ratio

The ratio of new visible edges (e) and ratio of average gradient ($\bar{r}$) are also utilized to monitor the performances of the proposed approach. The e represents the improved rate of visible edges of haze free images, and is calculated as follows [21]:

$$e = \frac{n_k - n_l}{n_l} \tag{16}$$

where n_k and n_l represents the cardinal number of the visible edges in the hazy image I_κ and the haze free image O_p, respectively.

The maximum e states that the edges of haze free image are stronger. The $\bar{r}$ utilizes the gradients of visible edges in the haze free image, to depict the restoration degree of the image edge and texture information. $\bar{r}$ is described as follows:

$$\bar{r} = e^{\left[\frac{1}{n_k} \sum\limits_{i \in \phi_k} log r_i\right]} \tag{17}$$

where $r_i = \frac{\Delta k}{\Delta l}$, k and l are the gradients of Δk and Δl, respectively, r_i denotes the set of visible edges of O_p. A maximum $\bar{r}$ state that the corresponding dehazing technique has improved capacity of edge preservation than others.

6.2.4 Perceptual haze density

An effective technique for haze density prediction is discussed in [7] in which the input image is divided into $N \times N$ sections and aggregate average values are computed. All $N \times N$ sections are utilized to evaluate various haze aware features such as variance, sharpness, contrast energy, image entropy, dark channel prior, color saturation, colorfulness etc. Mahalanobis-like measure [46] is applied on these features to evaluate the Multivariate Gaussian (MVG) fit of n dimensions can be mathematically calculated as follows:

$$P(s) = \frac{1}{\sqrt{(2\pi)^n |D|}} exp\left(-0.5 * (s-\mu)^t C^{-1} (s-\mu)\right) \tag{18}$$

Here, s denotes the haze aware statistical features, μ represents mean and $n \times n$ demonstrates the covariance matrix of different hazy features. Also, D represents determinant and C^{-1} depicts the covariance matrix inverse for MVG. D and C^{-1} can be derived using maximum

likelihood (ML) estimation [11]. Next, Mahalanobis-like distance can be calculated as follows:

$$D = \sqrt{(m_1 - m_2)^t \left(\frac{C_1 + C_2}{2}\right)^{-1} (v_1 - v_2)} \tag{19}$$

where, m_1 and m_2 are mean vectors and C_1 and C_2 are covariance matrices for MVG model of the haze free corpus and MVG fit of the test image.

Another metric L_f which has haze free level of the test haze image is calculated which is the distance norm of MVG versus haze aware statistical features. This information is extracted from a haze test image and normal MVG model from a group of 500 hazy images [7]. Afterwards haze density D can be calculated calculated as follows:

$$D_h = \frac{D}{1 + L_f} \tag{20}$$

Values of D_h are proportional to the corresponding haze density.

7 Significance and benefits to society

Haze removal techniques play an important role in vision processing applications. Subsequent section briefly explains some of the most significant applications in which haze removal techniques are utilized.

7.1 Airplanes

Generally, takeoff and landing of airplanes become challenging task in hazy environment. Many flights get delayed or some times are canceled due to hazy environment. To handle this issue, one can use haze removal algorithms to make the perceived scene as haze free.

7.2 Underwater image processing

For researchers and divers, it is hard to attain maximum information from underwater images. Like during shark attack, underwater scene analysis, etc. [37].

7.3 Remote sensing

Remotely sensed images play an important role in vision processing application. Due to high difference in camera and scene, haze will be introduced in the captured scene. Such as weather forecasting, detection of some particular objects demands haze free images[34].

7.4 Intelligent transportation vision system

In hazy days, due to poor visibility of roads, many accidents occurs on highways, especially in hilly areas. So, in order to prevent accidents on highways and hilly areas a haze removal technique is required to provide haze free image to driver using some visual equipment etc.

However, due to high speed of vehicles, it needs a haze removal technique with constant time complexity [23].

7.5 Intelligent railway

Many trains get delay or some times even canceled due to hazy environment. So, in order to handle this issue, one can use haze removal algorithms to make the perceived scene as haze for train drivers.

8 Conclusion and future work

In this paper, evolution of techniques for removal of haze from hazy images has been studied. Framework and challenges for the haze removal techniques have been discussed. Here, haze models have been studied which discovered the cause of poor visibility of the hazy image due to haze. Several features of the existing haze removal techniques are explored to encourage further research. Removal of the haze from single image is an difficult task because depth map is required to be estimated. Therefore, haze removal techniques demand certain constraints or prior knowledge. It is essential that during recovery of hazy image, both the illuminate and color characteristics should be restored in efficient way to preserve the color fidelity and appearance. Hence, future research will center on optimistic estimation of depth map and restoration parameters with better visual quality by using meta-heuristic techniques. A fast and optimistic monitoring of the depth information improves the speed and perceptual image quality.

References

1. Amintoosi M, Fathy M, Mozayani N (2011) Video enhancement through image registration based on structural similarity. The Imaging Science Journal 59(4):238–250
2. Cai B, Xu X, Jia K, Qing C, Tao D (2016) Dehazenet: an end-to-end system for single image haze removal. IEEE Trans Image Process 25(11):5187–5198
3. Chen BH, Huang SC, Ye JH (2015) Hazy image restoration by bi-histogram modification. ACM Transactions on Intelligent Systems and Technology (TIST) 6(4):50
4. Chen BH, Huang SC, Cheng FC (2016) A high-efficiency and high-speed gain intervention refinement filter for haze removal. J Disp Technol 12(7):753–759
5. Chen C, Do MN, Wang J (2016) Robust image and video dehazing with visual artifact suppression via gradient residual minimization. In: European conference on computer vision. Springer, pp 576–591
6. Cheng FC, Cheng CC, Lin PH, Huang SC (2015) A hierarchical airlight estimation method for image fog removal. Eng Appl Artif Intell 43:27–34
7. Choi LK, You J, Bovik AC (2015) Referenceless prediction of perceptual fog density and perceptual image defogging. IEEE Trans Image Process 24(11):3888–3901
8. Cozman F, Krotkov E (1997) Depth from scattering. In: Proceedings of the 1997 IEEE computer society conference on computer vision and pattern recognition, 1997. IEEE, pp 801–806
9. Ding M, Tong R (2013) Efficient dark channel based image dehazing using quadtrees. Science China Information Sciences 56(9):1–9
10. Ding M, Wei L (2015) Single-image haze removal using the mean vector l2-norm of rgb image sample window. Optik-International Journal for Light and Electron Optics 126(23):3522–3528
11. Duda RO, Hart PE, Stork DG (2012) Pattern classification. Wiley, New York
12. Fan X, Wang Y, Tang X, Gao R, Luo Z (2016) Two-layer gaussian process regression with example selection for image dehazing. IEEE Transactions on Circuits and Systems for Video Technology PP(99):1–1

13. Fang F, Li F, Yang X, Shen C, Zhang G (2010) Single image dehazing and denoising with variational method. In: 2010 IEEE international conference on image analysis and signal processing (IASP), pp 219–222
14. Fattal R (2008) Single image dehazing. ACM transactions on graphics (TOG) 27(3):72
15. Fattal R (2014) Dehazing using color-lines. ACM Transactions on Graphics (TOG) 34(1):13
16. Fu Z, Yang Y, Shu C, Li Y, Wu H, Xu J (2015) Improved single image dehazing using dark channel prior. J Syst Eng Electron 26(5):1070–1079
17. Galdran A, Vazquez-Corral J, Pardo D, Bertalmío M (2015) Enhanced variational image dehazing. SIAM Journal on Imaging Sciences 8(3):1519–1546
18. Galdran A, Vazquez-Corral J, Pardo D, Bertalmío M (2017) Fusion-based variational image dehazing. IEEE Signal Processing Letters 24(2):151–155
19. Ge G, Wei Z, Zhao J (2015) Fast single-image dehazing using linear transformation. Optik-International Journal for Light and Electron Optics 126(21):3245–3252
20. Guo F, Peng H, Tang J (2016) Genetic algorithm-based parameter selection approach to single image defogging. Inf Process Lett 116(10):595–602
21. Hautiere N, Tarel JP, Aubert D, Dumont E (2011) Blind contrast enhancement assessment by gradient ratioing at visible edges. Image Analysis & Stereology 27(2):87–95
22. He K, Sun J, Tang X (2011) Single image haze removal using dark channel prior. IEEE Transactions on Pattern Analysis and Machine Intelligence 33(12):2341–2353
23. Huang SC, Chen BH, Cheng YJ (2014) An efficient visibility enhancement algorithm for road scenes captured by intelligent transportation systems. IEEE Trans Intell Transp Syst 15(5):2321–2332
24. Kaufman Y, Tanré D, Gordon H, Nakajima T, Lenoble J, Frouin R, Grassl H, Herman B, King M, Teillet P (1997) Passive remote sensing of tropospheric aerosol and atmospheric correction for the aerosol effect. Journal of Geophysical Research: Atmospheres 102(D14):16,815–16,830
25. Kim JH, Jang WD, Sim JY, Kim CS (2013) Optimized contrast enhancement for real-time image and video dehazing. Journal of Visual Communication and Image Representation 24(3):410–425
26. Kumari A, Sahoo SK (2015) Fast single image and video deweathering using look-up-table approach. AEU-International Journal of Electronics and Communications 69(12):1773–1782
27. Lee S, Yun S, Nam JH, Won CS, Jung SW (2016) A review on dark channel prior based image dehazing algorithms. EURASIP Journal on Image and Video Processing 2016(1):4
28. Li Z, Zheng J (2015) Edge-preserving decomposition-based single image haze removal. IEEE Trans Image Process 24(12):5432–5441
29. Li J, Zhang H, Yuan D, Sun M (2015) Single image dehazing using the change of detail prior. Neurocomputing 156:1–11
30. Li Z, Zheng J, Zhu Z, Yao W, Wu S (2015) Weighted guided image filtering. IEEE Trans Image Process 24(1):120–129
31. Liu S, Rahman MA, Wong CY, Lin CF, Wu H, Kwok N et al (2017) Image de-hazing from the perspective of noise filtering. Comput Electr Eng 62:345–359
32. Ma Z, Wen J, Zhang C, Liu Q, Yan D (2016) An effective fusion defogging approach for single sea fog image. Neurocomputing 173:1257–1267
33. Narasimhan SG, Nayar SK (2002) Vision and the atmosphere. Int J Comput Vis 48(3):233–254
34. Pan X, Xie F, Jiang Z, Yin J (2015) Haze removal for a single remote sensing image based on deformed haze imaging model. IEEE Signal Processing Letters 22(10):1806–1810
35. Riaz I, Yu T, Rehman Y, Shin H (2016) Single image dehazing via reliability guided fusion. J Vis Commun Image Represent 40:85–97
36. Rong Z, Jun WL (2014) Improved wavelet transform algorithm for single image dehazing. Optik-International Journal for Light and Electron Optics 125(13):3064–3066
37. Serikawa S, Lu H (2014) Underwater image dehazing using joint trilateral filter. Comput Electr Eng 40(1):41–50
38. Singh D, Kumar V (2017) Dehazing of remote sensing images using improved restoration model based dark channel prior. The Imaging Science Journal 65(5):1–11
39. Singh D, Kumar V (2017) Modified gain intervention filter based dehazing technique. J Mod Opt 64(20):1–14
40. Singh D, Garg D, Singh Pannu H (2017) Efficient landsat image fusion using fuzzy and stationary discrete wavelet transform. The Imaging Science Journal 65(2):108–114
41. Sun W (2013) A new single-image fog removal algorithm based on physical model. Optik - International Journal for Light and Electron Optics 124(21):4770–4775
42. Sun W, Wang H, Sun C, Guo B, Jia W, Sun M (2015) Fast single image haze removal via local atmospheric light veil estimation. Comput Electr Eng 46:371–383

43. Tan RT (2008) Visibility in bad weather from a single image. In: IEEE Conference on computer vision and pattern recognition, 2008. CVPR 2008. IEEE, pp 1–8
44. Tarel JP, Hautiere N (2009) Fast visibility restoration from a single color or gray level image. In: 2009 IEEE 12th international conference on computer vision. IEEE, pp 2201–2208
45. Tripathi AK, Mukhopadhyay S (2012) Removal of fog from images: a review. IETE Tech Rev 29(2):148–156
46. Valls JM, Aler R, Fernández Ó (2005) Using a mahalanobis-like distance to train radial basis neural networks. In: Cabestany J, Prieto A, Sandoval F (eds) Computational intelligence and bioinspired systems: proceedings of the 8th international work-conference on artificial neural networks, IWANN 2005, Vilanova i la Geltrú, Barcelona, Spain, June 8-10, 2005. Springer, Berlin, pp 257–263. https://doi.org/10.1007/11494669_32. ISBN:978-3-540-32106-4
47. Wang YK, Fan CT (2014) Single image defogging by multiscale depth fusion. IEEE Trans Image Process 23(11):4826–4837. https://doi.org/10.1109/TIP.2014.2358076
48. Wang Z, Feng Y (2014) Fast single haze image enhancement. Comput Electr Eng 40(3):785–795
49. Wang L, Xiao L, Wei Z (2015) Image dehazing using two-dimensional canonical correlation analysis. IET Comput Vis 9(6):903–913
50. Wang R, Li R, Sun H (2016) Haze removal based on multiple scattering model with superpixel algorithm. Signal Process 127:24–36
51. Xie B, Guo F, Cai Z (2010) Improved single image dehazing using dark channel prior and multi-scale retinex. In: 2010 IEEE international conference on intelligent system design and engineering application (ISDEA), pp 848–851
52. Xie CH, Qiao WW, Liu Z, Ying WH (2016) Single image dehazing using kernel regression model and dark channel prior. SIViP 11(4):1–8
53. Xu H, Guo J, Liu Q, Ye L (2012) Fast image dehazing using improved dark channel prior. In: 2012 IEEE international conference on information science and technology. IEEE, pp 663–667
54. Yang HY, Chen PY, Huang CC, Zhuang YZ, Shiau YH (2011) Low complexity underwater image enhancement based on dark channel prior. In: 2011 2nd international conference on innovations in bio-inspired computing and applications (IBICA). IEEE, pp 17–20
55. Yang Y, Fu Z, Li X, Shu C, Li X (2013) A novel single image dehazing method. In: 2013 IEEE international conference on computational problem-solving (ICCP), pp 275–278
56. Zhao H, Xiao C, Yu J, Xu X (2015) Single image fog removal based on local extrema. IEEE/CAA Journal of Automatica Sinica 2(2):158–165
57. Zhu Q, Mai J, Shao L (2015) A fast single image haze removal algorithm using color attenuation prior. IEEE Trans Image Process 24(11):3522–3533

Dilbag Singh recieved the Master in Technology (Computer Science and Engineering) from Guru Nanak Dev University, Amritsar, Punjab, India (2012). Currenty, he is pursuing his Ph.D. degree in the field of image processing from Thapar University, Patiala, Punjab, India. He has published more than 11 research papers in well-known reputed journals and international conferences. His research interest includes Wireless sensor networks, Digital image processing and Meta-heuristic techniques.

Vijay Kumar received the B.Tech. from M.M. Engineering College, Mullana. He received M.Tech. from Guru Jambheshwer University of Science and Technology, Hisar. He has completerd his Ph.D. degree in Computer Engineering from National Institute of Technology, Kurukshetra. He has been an Assistant Professor with the Department of Computer Science and Engineering, Thapar University, Patiala. He has more than 8 years of teaching and research experience. He has more than 35 research papers in international journals, book chapters, and conference proceedings. His main research focuses on Soft Computing, Image Processing, Data Clustering and Multiobjective optimization.